

# ACCURACY ASSESSMENT OF VEGETATION MONITORING WITH HIGH SPATIAL RESOLUTION SATELLITE IMAGERY

RAFAEL WIEMKER, BORIS PRINZ, GERHARD MEISTER, RAMON FRANCK, HARTWIG SPITZER

II. Institut für Experimentalphysik, CENSIS  
Universität Hamburg

Mail: KOGS, Vogt-Kölln-Str. 30, 22527 Hamburg, Germany  
WWW: <http://kogs-www.informatik.uni-hamburg.de/projects/Censis.html>  
{wiemker,prinz,meister,franck}@kogs.informatik.uni-hamburg.de

**KEY WORDS:** Data Fusion, Multispectral Image Sharpening, High Resolution Satellites, Classification Accuracy

## ABSTRACT

For the years 1997 to 2000 it is expected that a number of new satellites will be launched into orbit by private companies which are specified to deliver panchromatic imagery of the earth surface with a spatial resolution as fine as 1 m. In contrast to the panchromatic band, the spectrally resolved bands will have a four times coarser ground resolution. Therefore, image fusion algorithms will be employed in order to produce panchromatic-'sharpened' color imagery.

The new satellites have the potential of stimulating and expanding the remote sensing market for image products at a resolution around one meter. In order to prepare for this era we have examined image fusion algorithms using already available airborne imagery. This paper describes tests of fusion algorithms on imagery which was simulated using multispectral images of an airborne scanner (DAEDALUS ATM) with an average pixel size of 1 m. The main advantage of this simulation of satellite images is the possibility to measure quantitatively the accuracy of the panchromatic-sharpened multispectral imagery. By comparison with the original airborne imagery, we evaluate the accuracy of the sharpened imagery with respect to the spectral signature, NDVI, local variance, and multispectral land cover classification.

## 1 HIGH RESOLUTION SATELLITE IMAGERY FOR LOCAL ENVIRONMENTAL MONITORING

For the years 1997 to 2000 it is expected that a number of new satellites will be launched into orbit by private companies (Doyle 1996, Fritz 1997) which are specified to deliver imagery of the earth surface of a spatial resolution as fine as 1 m.

This fine a resolution has so far been the privilege of airborne rather than spaceborne overhead imagery – at least as far as the civilian community and *multispectral* (in contrast to panchromatic) imagery is concerned. Airborne image flights have a longstanding importance for cadastre, local planning and local environmental monitoring (e.g. the health status of public trees in the city of Hamburg is monitored on aerial Color Infrared (CIR) photographs). So far the necessary image flights are conducted mostly by private enterprises on particular customer request. They are thus rather expensive.

Multispectral *spaceborne* imagery on the other hand has been exploited for a number of environmental issues (such as deforestation, desertification, plant stress, water pollution, climate warming etc.) but always on a *global* or *regional* scale – due to its limited spatial resolution (LANDSAT TM images have a pixel size of  $30 \times 30$  m).

With the arrival of meter-range spaceborne imagery which can be purchased off-the-shelf by local authorities at the instance when the demand arises, overhead imagery may become a serious option even for purposes of *local* interest which up to now could not justify the higher cost of a dedicated image flight.

## 2 SIMULATION OF HIGH RESOLUTION SATELLITE IMAGERY FROM MULTISPECTRAL AIRBORNE SCANNER IMAGERY

First image-recording of the announced satellites is expected for 1998. It can be assumed that the testing and calibration phase will last for the first year of operation. It has to be noted, however, that the schedule for all of the announced satellites already had to be delayed several times.

In the meantime, we are in the position to *simulate* the high resolution satellite imagery from airborne scanner images of comparable spatial resolution. The imagery was recorded by a DAEDALUS ATM line scanner with 10 spectral bands on board a Dornier Do 228 aircraft during five campaigns from 1991 to 1997 in cooperation with the German Aerospace Center (DLR Weßling / München) at flight altitudes of 300 m, 900 m and 1800 m. The 300 m imagery has a nadir-looking ground resolution of 70 cm. Due to the panorama characteristic of so-

SPACE IMAGING EOSAT IKONOS			DAEDALUS ATM	
Band		$\mu\text{m}$	Band	$\mu\text{m}$
Multispectral 4 m			Multispectral 1 m	
1	Blue	0.450–0.530	1	0.420–0.450
2	Green	0.520–0.610	2	0.450–0.520
			3	0.520–0.600
			4	0.605–0.625
			5	0.630–0.690
3	Red	0.640–0.720		
			6	0.695–0.750
4	NIR	0.770–0.880	7	0.760–0.900
			8	0.910–1.050
			9	1.550–1.750
			10	2.080–2.350
			Th.IR	8.500–13.000
Panchromatic 1 m				
	Pan	0.450–0.900		

Table 1: The expected spaceborne IKONOS spectral bands<sup>2</sup> and the actual airborne DAEDALUS spectral bands.

called ‘whisk broom’ - line scanners and the large swath angle of  $\pm 43^\circ$ , the ground resolution degrades to 1.4 m towards the image margins. Hence the images have a resolution of 1 m on average, in all 10 spectral bands.

For all environmental image analysis purposes it is essential to have a spectral band in the near infrared (NIR). There, vegetation has a very high reflectance and is the most distinct from non-vegetation land cover. Also, plant health and plant stress show up in the increase of reflectance between the red and the NIR. Therefore we have simulated photograph-like CIR images, where the spectral bands of Green, Red and the (invisible) Near Infrared (G,R,NIR) are coded by Blue, Green and Red (R,G,B), respectively, and merged into composite pseudo-color images.<sup>1</sup>

The specifications of the new high resolution satellites<sup>2</sup> (see Table 1 for an example) indicate that the 1 m resolution will only be reached for panchromatic imagery. The spectrally resolved bands will come in a spatial resolution of only 4 m.

We have simulated both the panchromatic full resolution image (by weighted average of the spectral bands), and the spectral band images (by averaging each  $4 \times 4$  pixel window into one new pixel). Results are shown in Fig. 1 for a small nature reserve near Nürnberg, Germany.



Figure 1: Simulated satellite product: Panchromatic image (top) of a small nature reserve around a lake near the airport of Nürnberg, resolution 1 m; and simulated color infrared MS<sub>4m</sub>-image<sup>1</sup> (bottom), resolution 4 m.

<sup>1</sup>Postscript and PDF versions of this paper containing the color images can be downloaded from <http://kogs-www.informatik.uni-hamburg.de/projects/censis/publications.html>

<sup>2</sup>Source: Space Imaging EOSAT (<http://www.spaceimaging.com>)

### 3 DATA FUSION BETWEEN 1 m PANCHROMATIC AND 4 m COLOR IMAGERY

For local environmental applications we need both the spectral resolution (i.e., at least three distinct spectral bands such as G,R,NIR) and good spatial resolution. Therefore, a fusion between the well resolved panchromatic and the four times coarser multispectral satellite images is necessary.

Numerous efforts have been made to fuse data received from the same scene by different sensors (see e.g. Shen et al. (1994), Darvishsefat (1995), Zhukov et al. (1995), Patterson et al. (1996), Peytavin (1996), Zhukov et al. (1996)). Particular respect has been paid to the merging of image data with differing spatial resolution. If the two sensors do not operate from the same platform, the geometric rectification and registration of the images is a prerequisite to data fusion. Experience has shown this to be a relatively easy process for satellite imagery (stable orbits and altitudes, small swath angles), but a rather cumbersome procedure for airborne line scanner imagery (flight track and altitude variations). In the particular case of the expected high resolution satellites this is not an issue since both the panchromatic and the multispectral image data are recorded from the same platform at the same time.<sup>2</sup>

#### 3.1 Interpolation of the MS<sub>4m</sub>-Imagery

The first step is the magnification of the 4 m pixel multispectral image by a factor 4 in order to yield a multispectral 4 m resolution MS<sub>4m</sub>-image with the same number of pixels as the panchromatic 1 m resolution PAN<sub>1m</sub>-image. This requires a resampling where the missing pixels are filled with nearest neighbor values, so that the resulting MS<sub>4m</sub>-image shows clearly the underlying 4 × 4 pixel structure (see Fig 1, lower image). Alternatively, using an interpolation scheme for computation of the missing pixels instead of using nearest neighbor values yields a much more satisfactory MS<sub>interp</sub>-image (see Fig. 3, top). For this paper we employed two-dimensional interpolation using tensor-product cubic B-splines (de Boor 1978).

#### 3.2 Fusion by IHS Transformation

An often applied fusion procedure is the merging of panchromatic with three-color RGB imagery in the IHS (or HSV) color space (Kraus 1990, Albertz 1991). The RGB image is transformed into Intensity, Hue, and Saturation; the Intensity is replaced by the high resolution panchromatic image; and then the image is transformed back into the RGB color space. This technique is known to work well for moderate resolution ratios (such as 1:3 for SPOT + LANDSAT TM, 10 m and 30 m). The results are still helpful but less reliable for resolution ratios such as 1:20, e.g. for fusion of SPOT color images with panchromatic aerial photography (Ersbøll et al. 1997). We note, however, that fusion by HSV transformation can be applied only to multispectral imagery consisting of three bands, since the image has to be coded as an RGB image before fusion can take place. Moreover, Prinz et al. (1997) have shown that the IHS-fusion results are clearly inferior to fusion using relative spectral contributions.

#### 3.3 Fusion by Relative Spectral Contributions

A simple fusion method which preserves the relative spectral contributions of each pixel but replaces its overall brightness by the high resolution panchromatic image works as follows:

$$(1) \quad \text{PSM}_{1m}^* = \text{MS}_{\text{interp}} \cdot \frac{\text{PAN}_{1m}}{\text{PAN}_{\text{interp}}} \quad (\text{for each pixel and each spectral band})$$

$$(2) \quad \text{PSM}_{1m} = \text{PSM}_{1m}^* \cdot \frac{\langle \text{MS}_{4m} \rangle}{\langle \text{PSM}_{1m}^* \rangle}$$

where PSM<sub>1m</sub> is the resulting panchromatic-sharpened multispectral 1 m image, MS<sub>interp</sub> is the cubic spline-interpolated image of a particular spectral band of the multispectral image set, PAN<sub>1m</sub> is the high resolution panchromatic image, and PAN<sub>interp</sub> is a panchromatic image created by averaging the three bands of the interpolated multispectral image MS<sub>interp</sub>.

The first equation describes the replacement of the coarse resolved panchromatic image PAN<sub>interp</sub> by the fine resolved panchromatic image PAN<sub>1m</sub>. Then, for each spectral band, the temporary result PSM<sub>1m</sub><sup>\*</sup> is adjusted such that the mean spectral value ⟨PSM<sub>1m</sub>⟩ of the final fusion result PSM<sub>1m</sub> is the same as the mean ⟨MS<sub>4m</sub>⟩ for the spectral band of the original MS<sub>4m</sub>-image.

In the first equation the quantity MS<sub>interp</sub>/PAN<sub>interp</sub> describes the relative contribution of each spectral band to the overall brightness of a pixel. This relative contribution, i.e., the chromatic information, is preserved by the multiplication with the spatially better resolved panchromatic PAN<sub>1m</sub>-image.

The result of an application of this technique to the exemplary image shown here can be seen in Fig. 3 (lower image).

#### 3.4 Spectral Class Specific Fusion

The simple fusion method described above can be refined by a modification of equation (2). First the original coarsely resolved multispectral MS<sub>4m</sub>-image is classified into *k* spectral classes using an unsupervised *k*-means clustering algorithm (Richards 1993, Wiemker 1997). The alignment of the mean spectral values is then carried out for each spectral band and each spectral class ω<sub>*c*</sub> individually (*c* = 1 . . . *k*). Let *r<sub>i</sub>*(*x<sub>c</sub>*) be the reflectance value of spectral band *i* for a specific pixel *x<sub>c</sub>* ∈ ω<sub>*c*</sub> belonging to class ω<sub>*c*</sub>. Then the reflectance values are aligned to the mean value ⟨*r<sub>i</sub>*(MS<sub>4m</sub>)⟩<sub>*c*</sub> of their specific spectral class ω<sub>*c*</sub>:

$$(3) \quad r_i(\text{PSM}_{1m}) = r_i(\text{PSM}_{1m}^*) \cdot \frac{\langle r_i(\text{MS}_{4m}) \rangle_c}{\langle r_i(\text{PSM}_{1m}^*) \rangle_c}$$

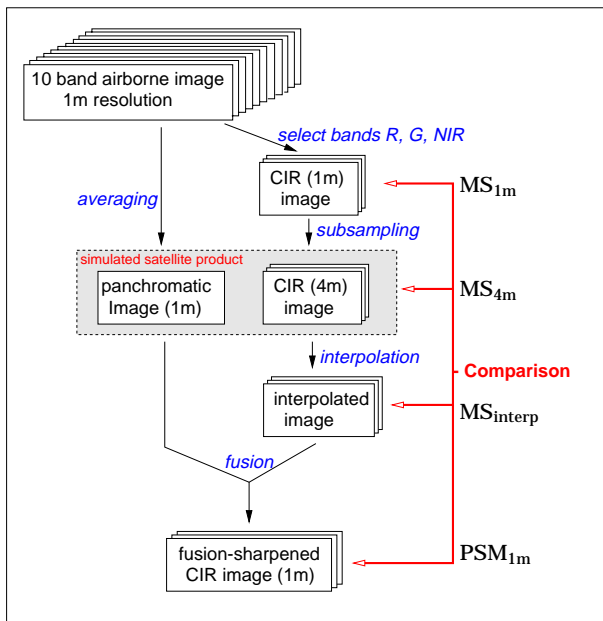


Figure 2: Simulation of the satellite imagery, image fusion, and comparison with the true 1 m imagery.

#### 4 COMPARISON BETWEEN FUSED IMAGE AND FULL-RESOLUTION IMAGE

Although the result of the fusion-sharpening appears surprisingly sharp and very satisfactory to the eye, its spectral truth remains to be checked quantitatively.

When the real satellite imagery becomes available, data fusion in order to yield highly resolved color images will certainly be performed. However, the accuracy of the estimated color values will remain unknown, and thus also the errors which propagate through later image processing steps such as land cover classification, change detection, NDVI computation, etc.

In contrast, with the airborne / simulated imagery we are in a position to immediately check the deviation between the multispectral imagery which is truly sampled with 1 m ground resolution and the one interpolated from 4 m resolution by data fusion with 1 m panchromatic resolution.

The flow chart in Fig. 2 shows the steps involved in the simulation of the panchromatic and color infrared images, the fusion and the comparison.

##### 4.1 Spectral Accuracy of the Fused Image

We compare the reflectance values  $r_i$  of the spectral bands  $i \in \{NIR, R, G\}$  of the fusion-sharpened  $PSM_{1m}$ -image with the color infrared  $MS_{1m}$ -image which is truly sampled at 1 m. In Fig. 4 the correlation between the  $MS_{1m}$ -image and the fused  $PSM_{1m}$ -image is shown for the bands Near Infrared, Red and Green. Each pixel defined by its spatial coordinates has two reflectance values, one in the original and one in the fused image, so every point in the scatter plot represents one pixel. If both images were identical, all the points would be lo-

cubic spline-interpolated CIR image ( $MS_{interp}$ ) :



fusion-sharpened CIR image ( $PSM_{1m}$ ) :

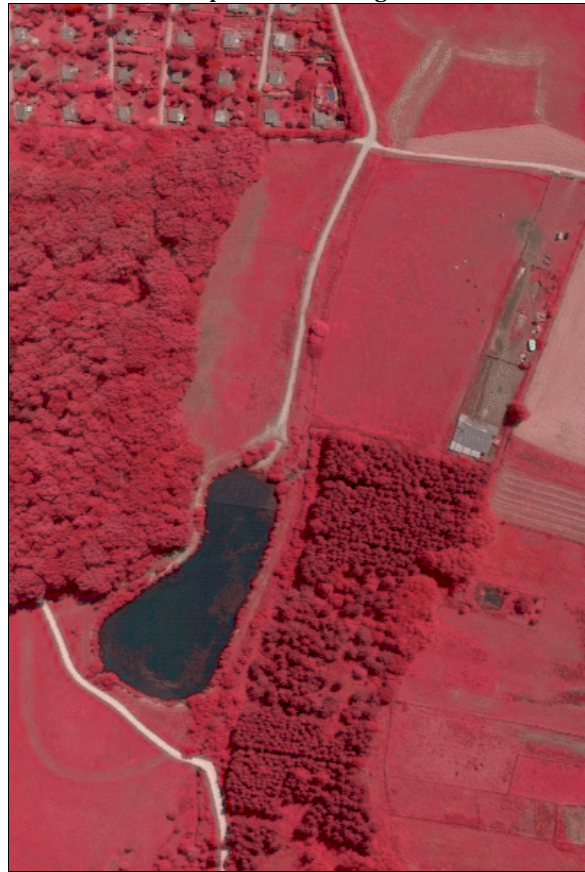


Figure 3: The cubic spline-interpolated CIR image<sup>1</sup> and the final fusion-sharpened CIR image<sup>1</sup> from panchromatic image (1 m) and interpolated color infrared image (4 m).

cated on the straight line which is also plotted for orientation. The correlation values and the mean deviation of the fusion-sharpened from the true 1 m reflectance values are given in Table 2.

While the correlation between both images is very good (97%) in the red and green bands, the near infrared seems to be less correlated (93%) for the simple fusion algorithm. In the scatter plot (Fig. 4, top left) it is obvious that there exist different spectral clusters which need specific alignment factors in order to preserve the mean reflectance value of the original MS<sub>4m</sub>-image. Application of the class-specific fusion algorithm (section 3.4) then indeed improves the spectral truth significantly (see Fig. 4, lower half, and Table 2).

## 4.2 Normalized Difference Vegetation Index

The normalized difference vegetation index (NDVI) is a feature of great importance for vegetation monitoring. It is defined as

$$\text{NDVI} = \frac{\text{NIR} - \text{R}}{\text{NIR} + \text{R}} \in [-1, +1]$$

where NIR is the near infrared band and R is the red band. It is obvious that the NDVI depends only on the relative relation of the spectral reflectance values and is thus invariant to scaling factors applied to all spectral bands. The panchromatic sharpening which preserves the relative spectral contributions thus does not affect the NDVI values. The NDVI depends on the chromatic information only, and cannot profit from additional panchromatic data of higher resolution. Still, the comparison of the NDVI values of the coarse 4 m MS<sub>4m</sub>-image and the fine 1 m MS<sub>1m</sub>-image shows a correlation of > 90% (Table 2).

## 4.3 Local Spectral Variance

Particularly for the classification of vegetation it is useful to consider texture features. One of the simplest texture features is the spectral variance in the local neighborhood  $\mathcal{N}(x)$  of a pixel  $x$ . Here we compute the root mean variance from all neighboring pixels  $x' \in \mathcal{N}(x)$  around  $x$  as

$$\sqrt{\frac{1}{3N} \sum_i \sum_{x' \in \mathcal{N}(x)} g(|x' - x|) [r_i(x') - \langle r_i(x') \rangle]^2}$$

for the three spectral bands  $i \in \{\text{NIR}, \text{R}, \text{G}\}$ , where  $\langle r_i(x') \rangle$  is the weighted mean value in the neighborhood  $\mathcal{N}(x)$ , using a Gaussian weighting  $g(|x' - x|)$  as a function of the distance  $|x' - x|$  of each neighboring pixel  $x'$  to the central pixel  $x$ , and a normalization factor  $N = \sum_{x' \in \mathcal{N}(x)} g(|x' - x|)$ . For the distance weighting we choose a Gaussian distribution width of  $\sigma = 1.83$  pixel, so that the influence is vanishing outside an  $11 \times 11$  pixel window.

As an example, the local spectral variance is high for forest areas, lower for meadows, and low for water and smooth artificial surfaces such as parking lots. In general the texture is highly correlated through the spectral bands, and thus captured well in the panchromatic band.

Therefore we find that this feature improves dramatically by the fusion-sharpening (Table 2). After fusion, the correlation with the true, 1 m resolved local spectral variance is > 90%.

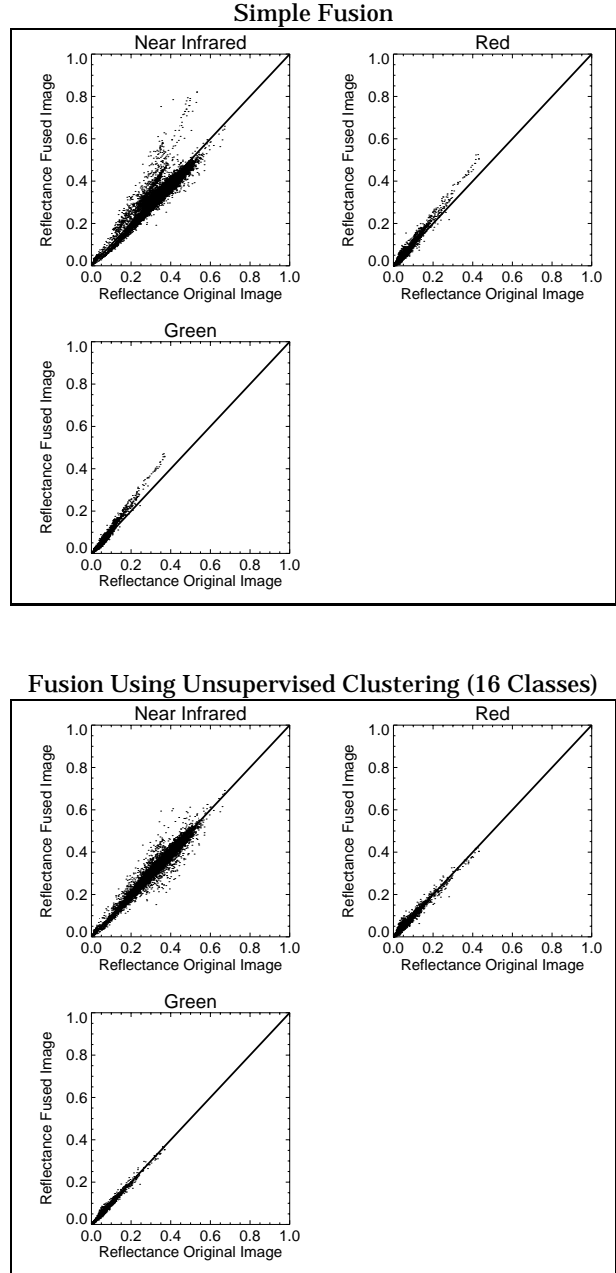


Figure 4: Scatter plots comparing the reflectance values of the true 1 m MS<sub>1m</sub>-image and the panchromatic-sharpened multi-spectral image for two fusion algorithms (Sections 3.3 and 3.4). The corresponding correlation values are given in Table 2.

## 5 CLASSIFICATION

One of the most wide-spread applications for multispectral images is ground cover classification. The classification of all image pixels into  $k$  classes can e.g. be performed by virtue of the spectral distance between the spectrum of a given pixel and the class reference spectra. In particular for images of vegetated areas it is also of interest to classify by virtue of derived features such as the NDVI, the NIR-reflectance and the local spectral variance. These three features were used for the following check of the classification accuracy of the sharpened PSM<sub>1m</sub>-imagery in comparison to the coarser MS<sub>4m</sub>-imagery.

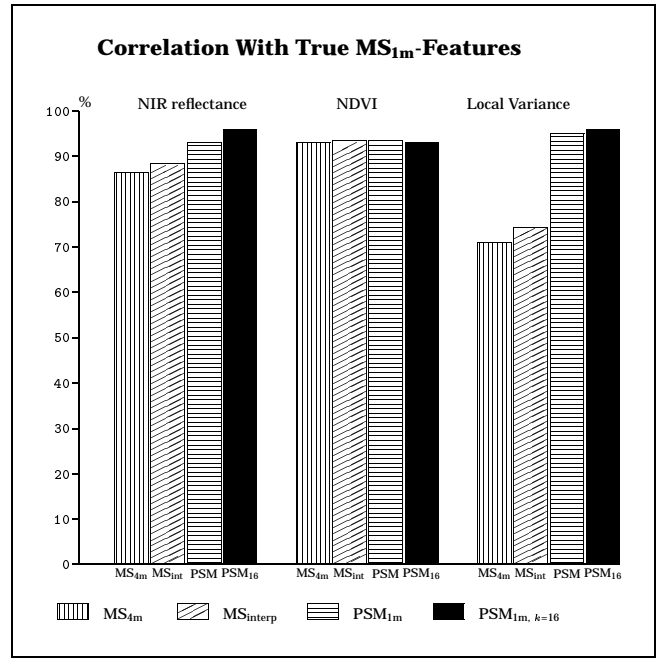
The accuracy of a land cover classification with respect to the ground truth is described by virtue of the kappa coefficient  $\kappa \in [-1, +1]$  (Congalton 1991, Richards 1993). The kappa coefficient is  $\kappa = 0$  for the pure coincidence between two totally random classifications, and reaches  $\kappa = 1$  for complete agreement between classification and ground truth. In our case, we consider the classification result of the 1 m multispectral MS<sub>1m</sub>-image as ground truth, and compute the kappa coefficient for the simulated spaceborne MS<sub>4m</sub>-image and for the fusion-sharpened PSM<sub>1m</sub>-image. The MS<sub>1m</sub>-, MS<sub>4m</sub>- and PSM<sub>1m</sub>-images were classified by the Minimum Euclidean Distance method with the same reference spectra for  $k = [2 \dots 12]$  classes. The reference spectra were established by unsupervised  $k$ -means clustering (Richards 1993, Wiemker 1997). The resulting classification accuracy kappa coefficients are plotted in Fig. 5, top.

Generally, the kappa coefficient decreases with increasing number of classes; i.e., the finer the classes are chosen, the higher the probability of mis-classification becomes. With respect to the fusion sharpening, however, we observe a significant increase of the classification accuracy for the fusion-sharpened PSM<sub>1m</sub>-image compared to the coarser MS<sub>4m</sub>-image, particularly for a higher number of classes  $k$ .

### 5.1 Land Cover Area Assessment

The results of land cover classification are often expressed in terms of the total area covered by a certain ground cover class, or a group of ground cover classes (e.g. the area of sealed surface, vegetated surface, building occupied surface etc.). Therefore it is of interest to measure how large the errors in land cover area assessment are: according to classification of the coarse MS<sub>4m</sub>-image, and according to classification of the sharpened PSM<sub>1m</sub>-image, both compared to the classification of the true 1 m resolved multispectral MS<sub>1m</sub>-image.

The results in Fig. 5, bottom, show the mean deviation from the land cover areas as assessed from the true 1 m resolved MS<sub>1m</sub>-image as percentages of the area of the whole scene. We see that for more than  $k = 6$  ground cover classes, the error in area assessment is originally at  $\approx 3\%$  and cut down to half by the fusion-sharpening.



COMPARISON TRUE VS. FUSED IMAGE

		MS <sub>4m</sub>	MS <sub>interp</sub>	PSM	PSM <sub>16</sub>
NIR reflectance					
$\in [0, 1]$	mean dev.	0.0441	0.0419	0.0305	0.0228
	correlation	86.6%	88.4%	93.2%	96.3%
Red reflectance					
$\in [0, 1]$	mean dev.	0.0103	0.0099	0.0067	0.0063
	correlation	87.2%	90.4%	97.1%	97.3%
Green reflectance					
$\in [0, 1]$	mean dev.	0.0103	0.0099	0.0067	0.0045
	correlation	86.4%	89.5%	97.4%	98.2%
NDVI					
$\in [-1, +1]$	mean dev.	0.054	0.053	0.056	0.054
	correlation	93.0%	93.6%	93.5%	93.3%
root mean local variance					
$\in [0, 0.5]$	mean dev.	0.0168	0.0199	0.0049	0.0049
	correlation	71.1%	74.4%	95.0%	96.2%

MS<sub>4m</sub> : multispectral imagery with 4 m pixel size (GSD)  
MS<sub>interp</sub> : multispectral imagery interpolated to 1 m pixel size, using cubic B-splines  
PSM : panchromatic sharpened (fused) multispectral imagery  
PSM<sub>16</sub> : panchromatic sharpened multispectral imagery, fusion algorithm discriminating 16 spectral classes (unsupervised clustering)

Table 2: Comparison of spectral truth, NDVI, and local spectral variance between the original, the interpolated, and the fusion sharpened multispectral imagery. The truth is evaluated by checking against the 1 m resolution multispectral airborne imagery from which the expected satellite products were simulated.

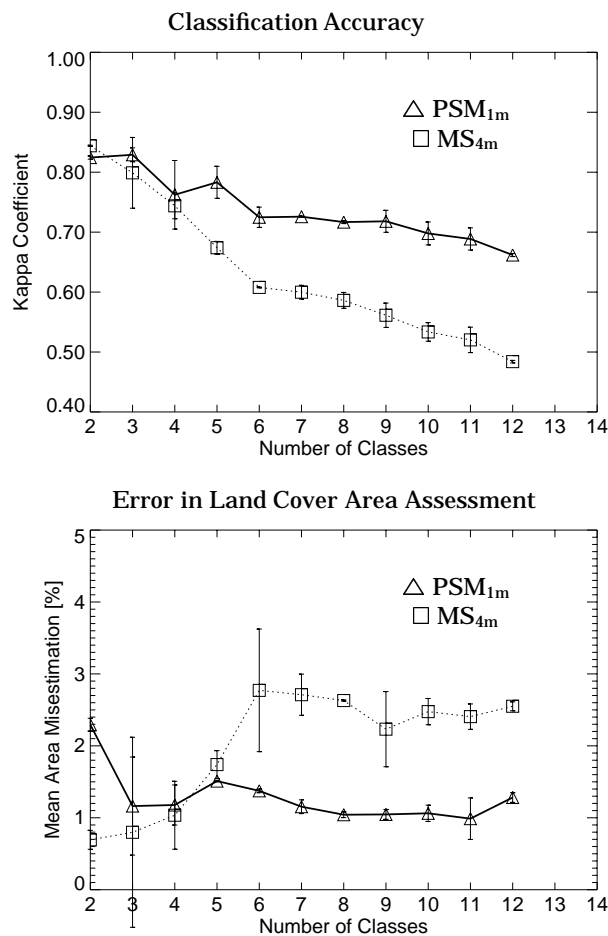


Figure 5: Classification accuracy (top), and error in land cover assessment (bottom) for the original MS<sub>4m</sub>-image (□) and the fusion-sharpened PSM<sub>1m</sub>-image (△). The error margins give the standard deviation from 4 different runs of unsupervised classification with random starting seeds.

## 6 CONCLUSIONS

High resolution satellite imagery (4 m multispectral and 1 m panchromatic, MS<sub>4m</sub> and PAN<sub>1m</sub>) was simulated using airborne scanner imagery with 1 m multispectral resolution (MS<sub>1m</sub>). Three different fusion algorithms were applied to the simulated data in order to obtain multispectral imagery sharpened by the higher resolved panchromatic band (panchromatic-sharpened multispectral imagery, PSM<sub>1m</sub>). The spectral truth of the sharpened PSM<sub>1m</sub>-imagery could be directly evaluated by comparison to the original airborne MS<sub>1m</sub>-imagery. Also derived features such as NDVI and local spectral variance could be compared between the original coarse, the fusion-sharpened and the true 1 m imagery. Finally the accuracy of land cover classification on the fusion-sharpened has been evaluated.

We could show that the panchromatic fusion sharpening does not only improve the eye appraisal of the images, but that it does also substantially improve the accuracy of the spectral reflectance values, and subsequent image classification.

The improvements have been quantified for an exemplary vegetation scene. Although the particular values do of course depend on the specific scene content, we consider the magnitude of the improvement obtained by the panchromatic sharpening as typical for MS<sub>4m</sub>/ PAN<sub>1m</sub>-fusion.

Findings of particular interest are:

- ▶ The MS<sub>interp</sub>-interpolation of the MS<sub>4m</sub>-image by cubic B-splines shows a slight improvement with respect to the spectral truth of the MS<sub>1m</sub>-image.
- ▶ Fusion preserving the relative spectral contributions (section 3.3) is significantly closer to the spectral truth than fusion by HSV-transformation (Prinz et al. 1997).
- ▶ The fusion by relative contributions is improved when the MS<sub>4m</sub>-image is first classified by unsupervised clustering and the fusion carried out separately for each spectral class (section 3.4). The class specific fusion improves specifically the accuracy of the NIR band. With this fusion method the correlation of  $\approx 85\%$  of MS<sub>4m</sub> is improved to  $\approx 95\%$  for the PSM<sub>1m</sub>. The mean deviation from the true reflectance values is diminished to approximately half.
- ▶ The feature NDVI of MS<sub>4m</sub> has a correlation of  $> 90\%$  with the true MS<sub>1m</sub>, and a mean deviation of only 0.05. The NDVI is not affected by the sharpening, since the relative contributions of the NIR and Red bands remain unchanged by the fusion method. Thus we have the same values for PSM<sub>1m</sub>.
- ▶ The local variance feature as the simplest texture feature is significantly improved by the fusion from  $\approx 75\%$  to  $\approx 95\%$  correlation with the true values.
- ▶ Comparing the results of unsupervised land cover classification on the MS<sub>4m</sub>-imagery and the sharpened PSM<sub>1m</sub> versus the true 1 m MS<sub>1m</sub>-imagery we find that the fusion improves the kappa-coefficients of classification truth by 20% (for the number of classes  $k > 6$ ) and reaches  $\kappa = 70\text{--}80\%$ .
- ▶ The error made in the assessment of the total area covered by a certain class is approximately cut to half and as small as  $< 1.5\%$  after fusion-sharpening.

## ACKNOWLEDGEMENT

This work was supported by the Volkswagen-Stiftung. The image flights were conducted in collaboration with the German Aerospace Center (DLR Weßling, München), particularly with the help of Volker Amann, Peter Hausknecht, Rudolf Richter and Manfred Schröder.

## REFERENCES

- Albertz, J. (1991). *Grundlagen der Interpretation von Luft- und Satellitenbildern*. Wissenschaftliche Buchgesellschaft, Darmstadt, 1991.
- Congalton, R. (1991). A Review of Assessing the Accuracy of Classifications of Remotely Sensed Data. *Remote Sensing of Environment* **37**, 35–46, 1991.
- Darvishsefat, A. A. (1995). Einsatz und Fusion von Multisensoralen Satellitendaten zur Erfassung von Waldinventuren. Technical report, University of Zurich, Department of Geography, Remote Sensing Series, vol. 24, 1995.
- de Boor, C. (1978). *A Practical Guide to Splines*. Springer, New York, 1978.
- Doyle, F. J. (1996). Thirty Years of Mapping from Space. In *Proceedings of the XVIII. Congress of the International Society for Photogrammetry and Remote Sensing ISPRS 1996, Vienna*, volume XXXI part B4 of *International Archives of Photogrammetry and Remote Sensing*, pages 227–230, 1996.
- Ersbøll, B.K., T.H. Nielsen, and K. Conradsen (1997). On Fusion of High (Spatial) Resolution Greyscale Imagery with Low (Spatial) Resolution Color Imagery. In *Proceedings of the Third International Airborne Remote Sensing Conference and Exhibition, Copenhagen*, Ann Arbor, 1997, volume II, page 337 (1 page). Environmental Research Institut of Michigan.
- Fritz, L.W. (1997). August 1997 Status of New Commercial Earth Observation Satellite Systems. In *Proceedings of the Joint Workshop of ISPRS WG I/1, I/3 and IV/4, Hannover, 29.IX.–2.X., Institute for Photogrammetry and Engineering Surveys, University of Hannover, 1998*, volume 17, pages 13–28, 1997.
- Kraus, K. (1990). *Fernerkundung, Band 2 – Auswertung photographischer und digitaler Bilder*. Dümmler, Bonn, 1990.
- Patterson, T.J., R. Haxton, M.E. Bullock, and S.B. Ulin-ski (1996). Quantitative Comparison of Multispectral Image-Sharpener Algorithms. In *Proc. SPIE – Int. Soc. Opt. Eng. (USA), Orlando*, volume 2758, pages 168–179, 1996.
- Peytavin, L. (1996). Cross-Sensor Resolution Enhancement of Hyperspectral Images Using Wavelet Decomposition. In *Proc. SPIE – Int. Soc. Opt. Eng. (USA), Orlando*, volume 2758, pages 193–203, 1996.
- Prinz, B., R. Wiemker, and H. Spitzer (1997). Simulation of High Resolution Satellite Imagery from Multispectral Airborne Scanner Imagery for Accuracy Assessment of Fusion Algorithms. In *Proceedings of the Joint Workshop of ISPRS WG I/1, I/3 and IV/4, Hannover, 29.IX.–2.X., Institute for Photogrammetry and Engineering Surveys, University of Hannover, 1998*, volume 17, pages 223–231, 1997.  
(<http://kogs-www.informatik.uni-hamburg.de/projects/censis/publications.html>).
- Richards, J. A. (1993). *Remote Sensing Digital Image Analysis*. Springer, Heidelberg, New York, 1993.
- Shen, S.S., J.E. Lindgren, and P.M. Payton (1994). Panchromatic Band Sharpening of Multispectral Image Data to Improve Machine Exploitation Accuracy. In *Proc. SPIE – Int. Soc. Opt. Eng. (USA), San Diego*, volume 2304, pages 124–131, 1994.
- Wiemker, R. (1997). Unsupervised Fuzzy Classification of Multispectral Imagery Using Spatial-Spectral Features. In Balderjahn, I., R. Mathar, and M. Schader, editors, *Classification, Data Analysis and Data Highways; Proceedings of the 21. Annual Meeting of the Gesellschaft für Klassifikation, GfKI'97, Potsdam, March 12–14, Heidelberg, 1997*, pages 101–109. Springer.  
(<http://kogs-www.informatik.uni-hamburg.de/projects/censis/publications.html>).
- Zhukov, B., M. Berger, F. Lanzl, and H. Kaufmann (1995). A New Technique for Merging Multispectral and Panchromatic Images Revealing Sub-Pixel Spectral Variation. In Stein, T.I., editor, *Proceedings of the International Geoscience and Remote Sensing Symposium, Florence, IGARSS 1995*, volume 3, pages 2154–2156. IEEE Catalog 95CH35770, 1995.
- Zhukov, B., D. Oertel, P. Strobl, F. Lehmann, and M. Lehner (1996). Fusion of Airborne Hyperspectral and Multispectral Images. In *Proc. SPIE – Int. Soc. Opt. Eng. (USA), Orlando*, volume 2758, pages 148–159, 1996.